atmosphere

MDPI

Article

Aerosol Types and Their Climatology over the Dust Belt Region

Ahmad E. Samman and Mohsin J. Butt *

Department of Meteorology, Faculty of Environmental Sciences, King Abdulaziz University, Jeddah 21589, Saudi Arabia; aesamman@kau.edu.sa
* Correspondence: mbutt@kau.edu.sa

Abstract: Aerosols, both natural and anthropogenic, are an important but complex component of the Earth's climate system. Their net impact on climate is about equal in magnitude to that of greenhouse gases but can vary significantly by region and type. Understanding and quantifying these aerosol effects is critical for accurate climate modeling and for developing strategies to mitigate climate change. In this paper, we utilize AERONET (Aerosol Robotic NETwork) data from 10 stations situated in the dust belt region to characterize aerosol properties essential for climate change assessment. Aerosol optical depth (AOD) data at 500 nm and Ångström exponent (α) data at the pair of wavelengths of 440 and 870 nm ($\alpha_{440\text{-}870}$) in the study region are analyzed to discriminate among different types of aerosols. The annual and monthly variabilities in AODs are analyzed to see the aerosols trend in the study region. In addition, the AOD and $\alpha_{440\text{-}870}$ data are utilized in order to determine different aerosol types during the period of study. Furthermore, the correlation coefficient between AODs and various meteorological parameters (temperature, wind speed, wind direction, relative humidity, and visibility) is analyzed. The results of the study indicate that Tamanrasset (2.49%), KAUST (1.29%), Solar Village (1.67%), and Dalanzadgad (0.64%) indicate an increasing trend, while Cairo (−0.38%), Masdar (−2.31%), Dushanbe (−1.18%), and Lahore (−0.10%) indicate a decreasing trend in AODs during the study period. Similarly, the results of characterizing aerosol types show that the highest percentage of desert dust aerosols (68%), mixed aerosols (86%), and biomass burning aerosols (15%) are found over Tamanrasset, Lahore, and Dalanzadgad AERONET stations. The study revealed a strong correlation between AODs and visibility, a moderate correlation with temperature, and a low correlation with other meteorological parameters (wind speed, wind direction, and relative humidity) in the study region. The results of the study are very encouraging and enhance our confidence in using historical AERONET data to improve our understanding of atmospheric aerosols' characteristics.

Keywords: AERONET; aerosol optical depth; dust belt; Ångström exponent

Citation: Samman, A.E.; Butt, M.J. Aerosol Types and Their Climatology over the Dust Belt Region. *Atmosphere* **2023**, *14*, 1610. https://doi.org/10.3390/atmos14111610

Academic Editor: Beatrice Moroni

Received: 29 September 2023
Revised: 20 October 2023
Accepted: 24 October 2023
Published: 27 October 2023

1. Introduction

Aerosols are tiny particles or droplets suspended in the air. These particles can be solid or liquid and are often so small that they remain airborne for an extended period due to their low settling velocity. Aerosols can be naturally occurring, like dust, sea spray, and volcanic ash, or they can be generated by human activities, such as industrial processes, vehicle emissions, and the burning of fossil fuels. The composition and behavior of aerosol particles in various size modes (coarse particles (2.5–100 μm in diameter), accumulation (0.1–2.5 μm), Aitken (0.01–0.1 μm), and nucleation modes (less than 10 nm)) [1] have far-reaching implications for climate, visibility, cloud formation, and atmospheric chemistry. Understanding these modes and their characteristics is crucial for comprehending the broader impacts of aerosols on the Earth's climate and environment. Aerosols' optical properties play an important role in the radiation balance on a global scale. However, our knowledge regarding their effects in the assessments and prediction of global climate change is considerably limited to date [2,3]. In order to precisely measure this aspect of

climate forcing (for example, surface irradiance), there is an essential need for a thorough and long-term measurement/classification of the optical properties of aerosols that differ both in space and time [4–6].

The primary origins of natural aerosols are the dust belt [7], an extensive region extending from the western coast of North Africa, traversing through the Middle East [8,9], Central and South Asia [10,11], and reaching all the way to China [12,13]. The Sahara, the world's largest dust source, comprises several major dust origins in North Africa, including Tunisia and Northeast Algeria, the coastal region in Western Sahara and Western Mauritania, the Western Flanks of the Ahaggar Mountains, the Libyan Desert, the Bodele Depression, and the Nubian Desert covering parts of Egypt and Sudan [7,14,15]. The Middle Eastern deserts, notably those in Saudi Arabia (Rub' al Khali being the largest), Iraq, and Syria, constitute the second most significant dust source across the dust belt [16]. Similarly, in Asia, the primary natural dust contributors are deserts, like Kharan Desert, Thar Desert, Taklamakan Desert, and Gobi Desert [17–19]. Many of these dust sources are situated within topographic depressions characterized by extensive alluvial deposits, playas, and sand dunes [20].

The dust belt regions of North Africa, the Middle East, and Asia undergo remarkable seasonal shifts in dust activity, with each region experiencing its peak in different seasons. For example, the pattern in North Africa reflects the region's complex climatic dynamics as the dust activity peaks in the winter months in low latitudes and shifts gradually to higher latitudes as the year progresses, while the dust activity reaches its highest point in the Middle East during spring and summer, marked by increased dust emissions and transport, and the lowest in the winter, creating a clear seasonal contrast [7,13]. In Asia, dust levels surge dramatically in spring, but they decrease as the monsoon season arrives during summer, offering relief from dusty conditions [13]. These seasonal patterns highlight the dynamic nature of dust activity in these regions. When examining global trends in near-surface dust concentrations, excluding North America and Europe, there is an observed decrease of 1.2% per year from 1984 to 2012 [21]. The trend in North African dust concentration aligns closely with the global trend, while that in Northeast Asia exhibits a significant negative trend. In contrast, the Middle East and Southwest Asia show slightly positive dust concentration trends, with a notable decrease in dust concentration during the 1990s [21].

Satellite observations allow the widespread spatial coverage of an area but generally with a low temporal resolution due to orbital constrains [22–24]. In addition, the variables retrieved through satellite data are limited by errors due to a number of reasons, including underneath surface properties, aerosol detection model, and clouds that are associated with retrieved parameters [25]. In spite of the errors, satellite data undoubtedly have contributed enormously in order to understand the temporal and geographical variations in aerosol properties, particularly on a large scale. In contrast, ground-based measurements of atmospheric aerosols can be very valuable for the absolute and precise classification of aerosol optical properties. However, these observations are often limited in terms of spatial resolution. For example, global ground-based networks of sun-photometer, such as AERONET (AErosol RObotic NETwork), aim to provide a constant record of aerosol data, which are very important in order to establish the local, regional, and global climatology of aerosols' properties [24,26,27]. Communally, ground-based measurements of atmospheric aerosols also offer decisive data for the verification of satellite retrievals as well as model validations. Therefore, the measurement of the optical properties of the aerosols over any area is an important subject, particularly over the dust belt region.

Various researchers in different studies have considered aerosols' optical properties using ground-based AERONET data [24,27–31]. Kaskaoutis et al. (2012) [32] used AERONET data from the year 2001 to 2010 over northern India (Kanpur) in order to analyze the trend of and the variability in aerosols. They found that anthropogenic emissions increased over northern India during the study period. Similarly, using data from 14 sites of AERONET from North Africa and Arabian Peninsula [33] identified the dust optical properties over

study regions. They found that the effect of dust over the Arabian Peninsula is higher than that over northern Africa. In another study [34] used AERONET sites all over the world in order to estimate the concentration of black carbon as well as organic carbon (light-absorbing) in the atmosphere. They deduced that, during biomass-burning seasons, the columnar absorbing organic carbon level is higher over South America, China, and India compared to the US and Europe. Recently [24] validated a MODIS (moderate resolution imaging spectroradiometer) deep blue AOD (aerosol optical depth) product over Saudi Arabia with the help of AERONET station data and concluded that the concentration of AODs is very high over the eastern and northern regions of the country and, particularly, during the spring season between 2000 and 2013. They also suggested the deployment of more AERONET stations in the country in order to understand aerosols' variability with high precision. Similarly [27] applied the normalized difference dust index (NDDI) on MODIS data for sand storm monitoring (2002–2011) and validated their results using AERONET data. They emphasized the importance of AERONET data in dust-related research, particularly over Saudi Arabia.

This study attempts to enumerate the climatology and trends of and variability in the concentration of aerosols in the atmosphere at monthly and annual time scales using AERONET quality-assured (level 2) AOD data from 10 stations located in the dust belt region. The work presented in this study addresses the atmospheric aerosol concentration by analyzing the Ångström exponent and AODs for the study period. For this, the analysis of monthly and annual variations in aerosols (Ångström exponent and AODs) is performed. In the estimation of the Ångström exponent (linear fit of log λ versus log AODs), higher values indicate the presence of fine mode aerosols, especially due to anthropogenic pollution, whilst low values correspond to the existence of coarse aerosols, especially due to sand and dust (natural pollution) activities. The unique aspect of this study lies in its effective utilization of AODs and Ångström exponent ($\alpha_{440\text{-}870}$) data to discern and classify various aerosol types present during the study period. These datasets play a pivotal role in characterizing the composition and properties of aerosols within the atmosphere. By closely examining AODs and Ångström exponent values, distinct patterns and clusters emerge, facilitating the categorization of aerosols into different types. This analytical approach provides valuable insights into the origin, behavior, and characteristics of the aerosols observed in the study regions, enhancing our comprehension of atmospheric aerosol dynamics. Finally, the trends of AODs, temperature, wind speed, wind direction, relative humidity, and visibility are also assessed, and a correlation is determined between the aerosols and these meteorological parameters.

2. Study Area

The composition of aerosols in the atmosphere is extraordinarily complex due to a number of reasons, including sand and dust storm events and contribution from anthropogenic emissions in a region. In addition, the geographical location and physiography of the region also play a major role in the contribution of the atmospheric aerosols. Thus, the nature of aerosols in the atmosphere can be complex due to variabilities in the size, shape, and type of the atmospheric particles. This led us to choose data from 10 AERONET stations situated within the dust belt region, including 3 stations in North Africa and Asia and 4 stations in the Middle East, as shown in Figure 1. These stations typify the key aerosol characteristics found in different environments, including urban, desert, coastal, and biomass-burning regions. For example, among the three stations in Asia, the AERONET station in Dalanzadgad is located in the southern part of Mongolia and is surrounded by the arid landscapes of the Gobi Desert. The famous Khongor Sand Dunes, one of the iconic features of the Gobi Desert, are located relatively close to Dalanzadgad. The city experiences a cold desert climate, characterized by extreme temperature variations between summer and winter. The city has seen infrastructure development in recent years that includes improved transportation connections, accommodations, and amenities for people. This makes the city an interesting region in terms of both natural and anthropogenic aerosols in the atmosphere.

On the other hand, the remaining two stations in Asia, Lahore and Dushanbe, are among the largest metropolitan cities in Pakistan and Tajikistan, respectively. Lahore, which is one of the largest cities in Pakistan in terms of population, also experiences issues related to biomass burning, particularly during the months of October and November. In recent years, Lahore has experienced significant pollution, which, at times, originates from neighboring China and India and lingers over the city during the winter months. Dushanbe, the capital city of Tajikistan, is located in a valley along the Varzob River, enveloped by mountains. The city experiences a continental climate, marked by hot summers and cold winters, with the majority of its rainfall occurring in the spring and early summer, with July being the wettest month. Both the aforementioned urban areas are expected to have a higher concentration of anthropogenic aerosols, primarily from human activities as opposed to natural sources.

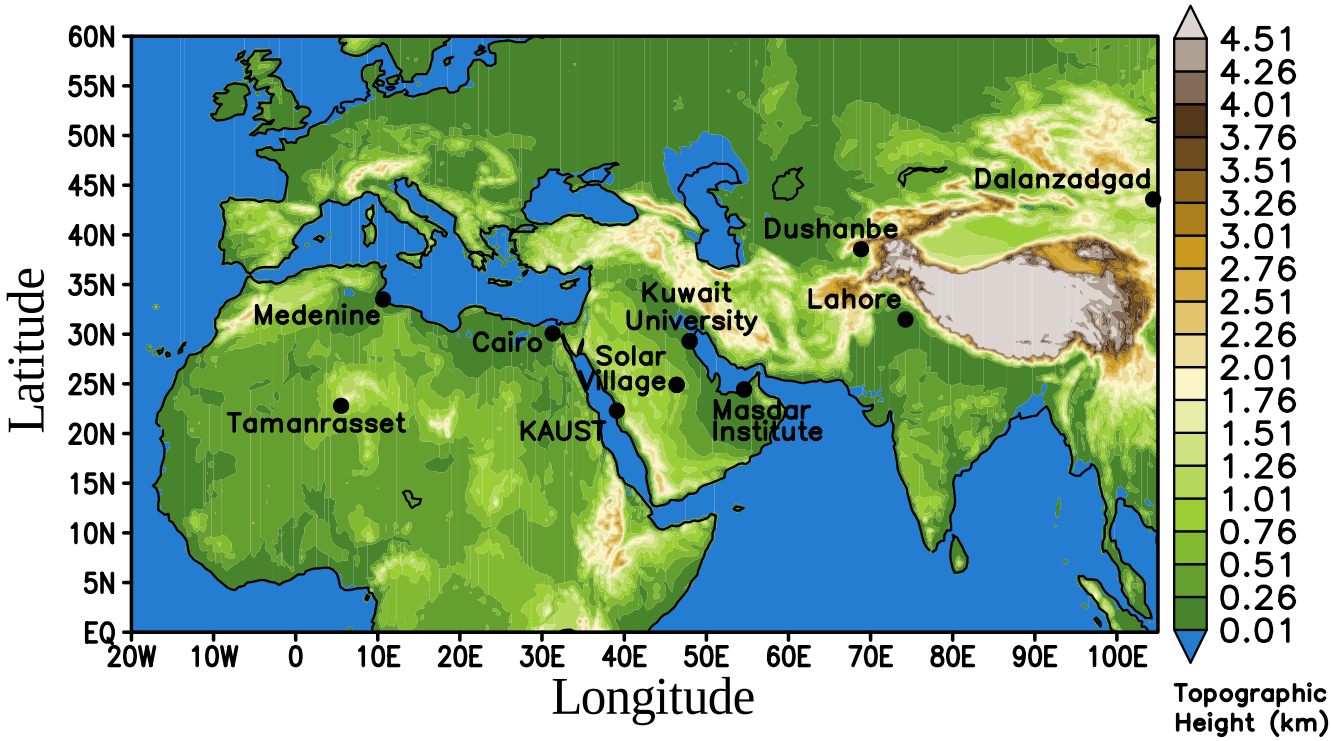

Figure 1. The topography (km) of the study region and the location of the AERONET stations.

Similarly, among the four stations in the Middle East, the AERONET stations at Kuwait University and Masdar Institute are in coastal and metropolitan regions, while the AERONET station at Solar Village is in a desert region, and the station at KAUST is in a coastal region. Kuwait City is located in the northeastern part of the Arabian Peninsula along the Arabian Gulf. The city experiences desert climate surrounded by arid desert and is located on a relatively flat terrain with minimal variation in elevation. Masdar Institute is located in the arid desert environment of the UAE. The region experiences a hot desert climate characterized by extremely high temperatures during the summer months and relatively mild winters. KAUST is situated on the coast of the Red Sea in Saudi Arabia surrounded by the arid landscapes of the Arabian Desert (sand dunes, rocky terrain, and minimal vegetation typical of desert regions). It experiences a desert climate with hot, arid summers and mild, relatively cooler winters. Solar Village is located in the heart of the Arabian Desert, which is characterized by vast stretches of arid, sandy terrain, rocky plateaus, and occasional desert vegetation adapted to arid conditions and experiences a hot desert climate.

Finally, among the three stations in North Africa, the AERONET station in Cairo is in a metropolitan city. Cairo, the capital and largest city of Egypt, is located in the northeastern corner of the African continent along the banks of the Nile River and experiences a hot

desert climate. The AERONET station in Medenine is located in southeastern Tunisia and is influenced by its proximity to the Mediterranean Sea and its location on the northern edge of the Sahara Desert, resulting in some variability in weather conditions throughout the year. The region can experience occasional strong winds, including hot and dry Sirocco winds, which originate from the Sahara Desert and can lead to dust and sand in the air. The AERONET station at Tamanrasset is in a desert region located in the southern part of Algeria, in the central Sahara Desert. It experiences a hot desert climate, characterized by extremely hot summers and relatively mild winters. The landscape around Tamanrasset is typical of the Sahara Desert, characterized by vast expanses of sand dunes, rocky plateaus, and desert vegetation adapted to arid conditions.

3. Data and Methodology

The spectral behavior of AODs is influenced by both natural and anthropogenic processes, making it a valuable parameter in the study of atmospheric aerosols. The ground-based Cimel sky radiometer has been operational in different parts of the world in collaboration with the NASA (National Aeronautics and Space Administration) AERONET network to measure atmospheric AODs. A detailed description of the Cimel Sun photometer, which is the integral instrument of the AERONET network, can be found in [26]. The instrument is a spectral radiometer measuring AODs at eight spectral bands (340 nm, 380 nm, 440 nm, 500 nm, 675 nm, 870 nm, 940 nm, and 1020 nm) with a 15 min temporal resolution working robotically to point towards sun and sky powered by solar energy and is weather-shielded [35]. Similarly, the Ångström parameter (α) can be computed based on measurements taken at different pairs of wavelengths (for example, $\alpha_{340\text{-}440}$, $\alpha_{380\text{-}500}$, $\alpha_{440\text{-}675}$, $\alpha_{440\text{-}870}$, and $\alpha_{500\text{-}870}$). All the measurements were performed using the instrument, whilst the data processing was performed within the AERONET standard procedures. An algorithm was used to obtain the AOD values (with an absolute error between 0.01 and 0.02) from the acquired data from the observations obtained from the Cimel sun photometer directly pointed towards the Sun. An additional AERONET standard cloud-screening algorithm was used in the case of cloud cover during the measurement hours [28].

Three different levels of AERONET data, that is, level 1, level 1.5, and level 2, are available and can be retrieved free of cost. Level 1 is unscreened data, level 1.5 is cloud-screened, and level 2 is quality-assured data. One of the most commonly used wavelengths for monitoring atmospheric aerosols is 500 nm. The values of AODs at 500 nm are indicative of turbid conditions and the aerosol type [36]. AERONET has a long history of measurements at 500 nm, making it a common reference wavelength for aerosol monitoring. This consistency enables researchers to compare and analyze data collected over many years. Thus, in the current study, we utilized AOD data to explore the annual and monthly variations in aerosol properties and potentially develop regional climatology for the ten chosen locations. We also attempted to characterize the aerosol types by using AODs and Ångström exponent ($\alpha_{440\text{-}870}$ data). Typically, the literature reports a wide range of patterns in AOD and Ångström exponent scatter plots (for example [37,38], making interpretation quite challenging. However, the comprehensive spectral data provided by the Ångström exponent can assist in identifying and distinguishing between various aerosol types in a specific geographic region. Hence, scatter plots between AODs and the exponent generated for 10 locations were used to identify distinct aerosol types for a particular location by identifying the physically interpretable cluster regions on the graph. Thus, in the current research, level 2 AERONET AOD data at a 500 nm wavelength and the Ångström exponent ($\alpha_{440\text{-}870}$) were retrieved from 10 different AERONET stations over the study region for the available period, as shown in Table 1, from the official website, available at http://aeronet.gsfc.nasa.gov, accessed on 1 June 2023.

In the current research, the relationship between AODs and the temperature, wind speed, wind direction, relative humidity, and visibility were also investigated over the study region. The meteorological data (METAR) of the aforementioned parameters used in the current study were retrieved from Iowa State University's Iowa Environmental Mesonet

(https://mesonet.agron.iastate.edu, accessed on 5 September 2023). First, the aerosols and meteorological parameters' hourly values were averaged and extracted over the ten AERONET sites. For this, we matched AERONET and meteorological points (10 stations) in a space and time window. The dates for which the meteorological parameters' data co-registered with the AERONET station data were extracted from the entire dataset and analyzed using a correlation coefficient.

Table 1. AERONET stations' information.

Station Name	Geographic Region	Country	Longitude	Latitude	Elevation (m)	Available Data
Tamanrasset	Northern Africa	Algeria	5.53	22.79	1377.0	2006–2022
Medenine	Northern Africa	Tunisia	10.64	33.5	33.5	2014–2015 2018–2020
Cairo	Northern Africa	Egypt	31.29	30.08	70.0	2010–2023
KAUST	Middle East	Saudi Arabia	39.10	22.30	11.2	2012–2023
Solar Village	Middle East	Saudi Arabia	46.39	24.90	764.0	1999–2015
Kuwait University	Middle East	Kuwait	47.97	29.32	42.0	2006–2012 2016–2022
Masdar Institute	Middle East	UAE	54.61	24.44	4.0	2012–2022
Dushanbe	Asia	Tajikistan	68.85	38.55	821.0	2010–2023
Lahore	Asia	Pakistan	74.26	31.48	209.0	2006–2023
Dalanzadgad	Asia	Mongolia	104.41	43.57	1470.0	1997–2023

4. Results and Discussion

4.1. AODs and Ångström Exponent Variability Climatology

Changes in AODs can have far-reaching consequences for climate, air quality, and public health. Understanding the magnitude of these changes is crucial for assessing their potential climate and environmental impacts on local and global scales. Therefore, the percentage change in AODs for each station was calculated and is presented in Table 2. This information is valuable for determining whether aerosol concentrations are increasing, decreasing, or remaining relatively stable in specific regions, which is essential for identifying areas with more significant fluctuations in aerosol levels compared to others.

In the current research, we utilized spectral AOD data to explore the fluctuations in aerosol characteristics and potentially develop a regional climatology for the ten chosen locations. Since the spectral shape of the extinction is related to the particle size, the Ångström exponent is generally used as a measure for the main aerosol size in the atmosphere at the time of observation [39–41]. Thus, in the current study, the mean annual and monthly AODs as well as the Ångström exponent ($\alpha_{440\text{-}870}$) for ten AERONET stations in the dust belt region, that is, North Africa (Tamanrasset, Medenine, and Cairo), Middle East (Sollar Village, KAUST, Kuwait University, and the Masdar Institute), and Asia (Dushanbe, Lahore, and Dalanzadgad), as shown in Figure 1, for different time periods, were analyzed and are discussed in the following sections.

Table 2. Percentage changes in AODs for each station (TA = Tamanrasse; ME = Medenine; CA = Cairo; KA = KAUST; SV = Solar Village; KU = Kuwait University; MA = Masdar; DU = Dushanbe; LA = Lahore; and DA = Dalanzadga) during the study period.

Year	TA	ME	CA	KA	SV	KU	MA	DU	LA	DA
1998										8.48
1999										8.48
2000					18.62					−1.71
2001					−24.31					−3.45
2002					3.03					
2003					17.48					
2004					−5.45					−12.15
2005					−5.83					10.70
2006					14.02					−1.10
2007	39.91				1.39	−12.55				−0.82
2008	19.68				14.94	41.23			−0.14	
2009	−42.30				−1.17	5.30			−19.21	
2010	−1.27				−23.75	2.51			24.74	10.42
2011	77.55		−3.94		35.70			0.17	−5.09	−5.94
2012	−11.71		−3.58		−2.30			−10.95	0.47	3.85
2013	−8.70		3.59	−8.79	−19.00		−24.21	1.16	−4.46	−8.95
2014	8.29		−2.80	−20.00			13.20	8.01	1.02	8.85
2015	11.68	−7.94	2.21	44.00			13.28	−14.53	2.11	−5.48
2016	−0.06		−0.54	−6.91			−10.82	9.08	−2.91	0.05
2017	−10.44		2.11	9.05			5.20	10.95	0.24	−1.51
2018	−7.70		4.41	−4.29			−4.09	−9.35	−17.98	−5.62
2019	5.18	44.93	−4.87	−18.03			−8.44	9.86	31.96	19.63
2020	−0.83	−19.65		6.69		−3.32	7.87	−16.16	−10.49	−9.66
2021	6.81			15.41		−0.50	−12.7712		−1.60	0.40
2022	−46.21			−57.01						−1.09
2023				54.07						

4.1.1. North Africa

The average annual AOD and Ångström exponent ($\alpha_{440\text{-}870}$) for the North African AERONET stations (Tamanrasset, Medenine, and Cairo) are shown in Figure 2a,b, while the average monthly AODs and Ångström exponent ($\alpha_{440\text{-}870}$) for the same stations are shown in Figure 3a,b. The average annual AOD (Ångström exponent) value for the Tamanrasset station is 0.29 (0.28) during the study period (2006–2022). It is evident from Figure 2a,b (black line) that the highest value of the annual AOD (Ångström exponent) for the Tamanrasset station is 0.36 (0.46) for the year 2011, while the lowest value of the annual AOD (Ångström exponent) is 0.18 (0.16) for the year 2022 (2014). In Tamanrasset city, high turbidity events occur annually from March to August due to the increased frequency of desert dust outbreaks, also referred to as the Saharan dust season (from March to June), and their transportation, which are also the main characteristics of the region. During these months, the Sahara Desert experiences strong winds, known as the Harmattan winds, which can lift large amounts of mineral dust and sand into the atmosphere [22,42]. This is clearly evident when examining the average monthly AOD (with high-value) and Ångström exponent (with low-value) data for the Tamanrasset station, as depicted by the black lines in Figure 3a,b, which is in agreement with previous research [43,44].

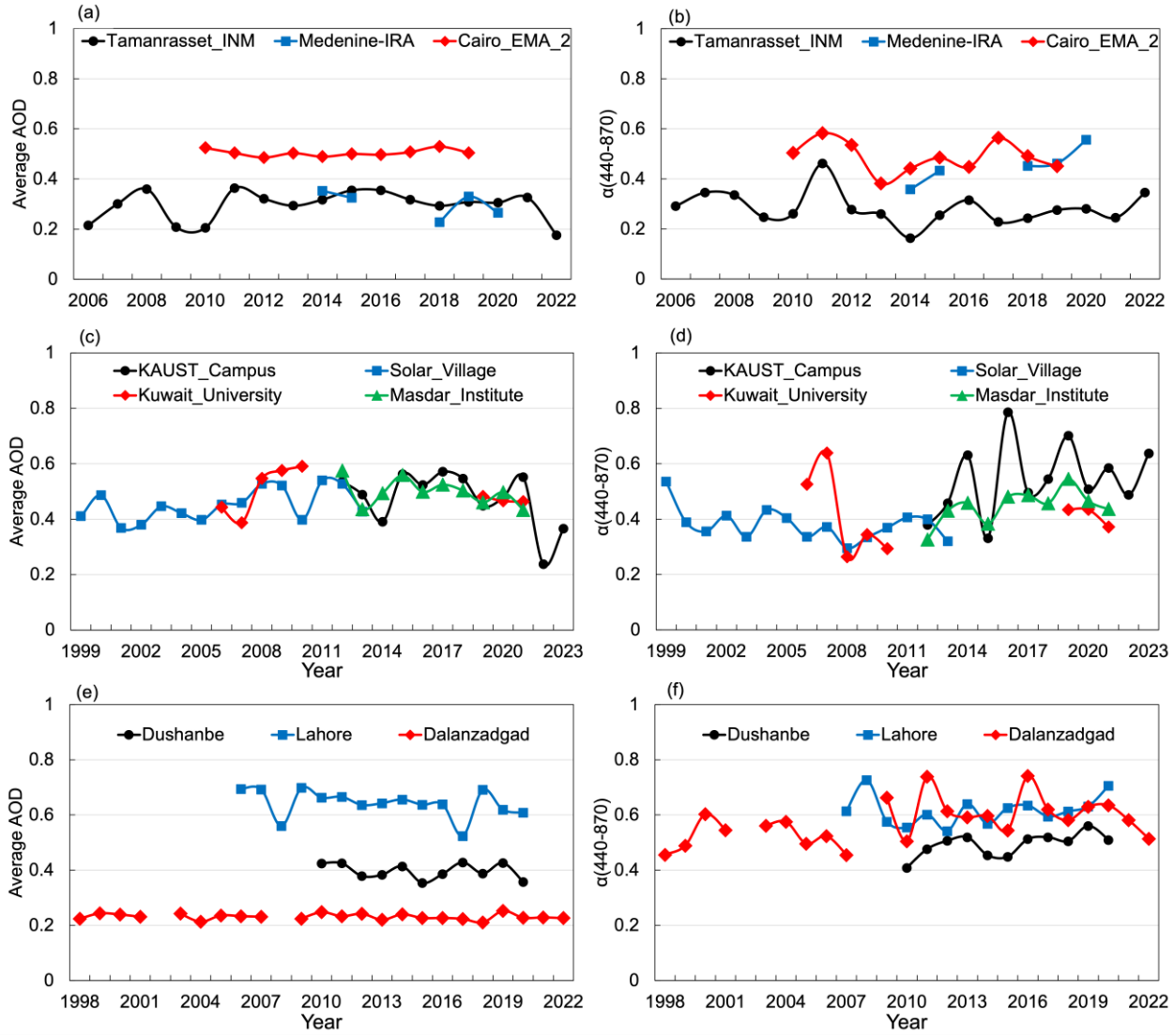

Figure 2. The average annual AOD and Ångström exponent ($\alpha_{440\text{-}870}$) (**a**,**b**) for North African (Tamanrasset, Medenine, and Cairo), (**c**,**d**) for Middle Eastern (KASUT, Solar Village, Kuwait University, and the Masdar Institute), and (**e**,**f**) for Asian (Dushanbe, Lahore, and Dalanzadgad) AERONET stations.

The average annual AOD (Ångström exponent) value for the Medenine station is 0.30 (0.45) over the study period (2014, 2015, and 2018–2020). It is evident from Figure 2a,b (blue line) that, for the Medenine station, the highest value of annual AOD (Ångström exponent) is 0.35 (0.56) for the year 2014 (2020), while the lowest value of annual AOD (Ångström exponent) is 0.23 (0.36) for the year 2018 (2014). The seasonal variations in aerosol concentrations in Medenine are influenced by several factors, including weather patterns, sources of aerosols, and regional climate. For example, spring (March, April, and May) can have relatively mild and stable weather conditions and aerosol levels may be lower, while summer (June, July, and August) is typically hot and dry and increased temperatures and dry conditions can lead to higher aerosol levels. In addition, dust and sand particles from nearby desert regions, such as the Sahara Desert, can be transported by the wind and contribute to elevated aerosol concentrations [22,45]. Furthermore, summer experiences occasional dust storms, which lead to significant spikes in aerosol levels. Similarly, autumn (September, October, and November) can be a transitional season with changing weather patterns. Aerosol levels may remain elevated from the summer, particularly if there are lingering dust particles in the atmosphere. However, winter (December, January, and February) tends to be cooler and can have occasional rainfall that helps to lower the aerosols

in the atmosphere. From the average monthly AOD analyses for the Medenine station (Figure 3a), the pattern of high AOD values in April and then from June to September is evident. This is evident when examining the average monthly AOD (with high-value) data for the Tamanrasset station, as depicted by the blue lines in Figure 3a, which indicates that the results align with what previous research has shown [44,46]. However, the pattern of low Ångström exponent (Figure 3b) is visible only during the months of June and July. This distinctive pattern may be attributed, in part, to the limited availability of AERONET data for the Medenine station, spanning only five years. With the small amount of data available for Medenine city, the monthly Ångström exponent figure may not reflect the exact aerosol variability.

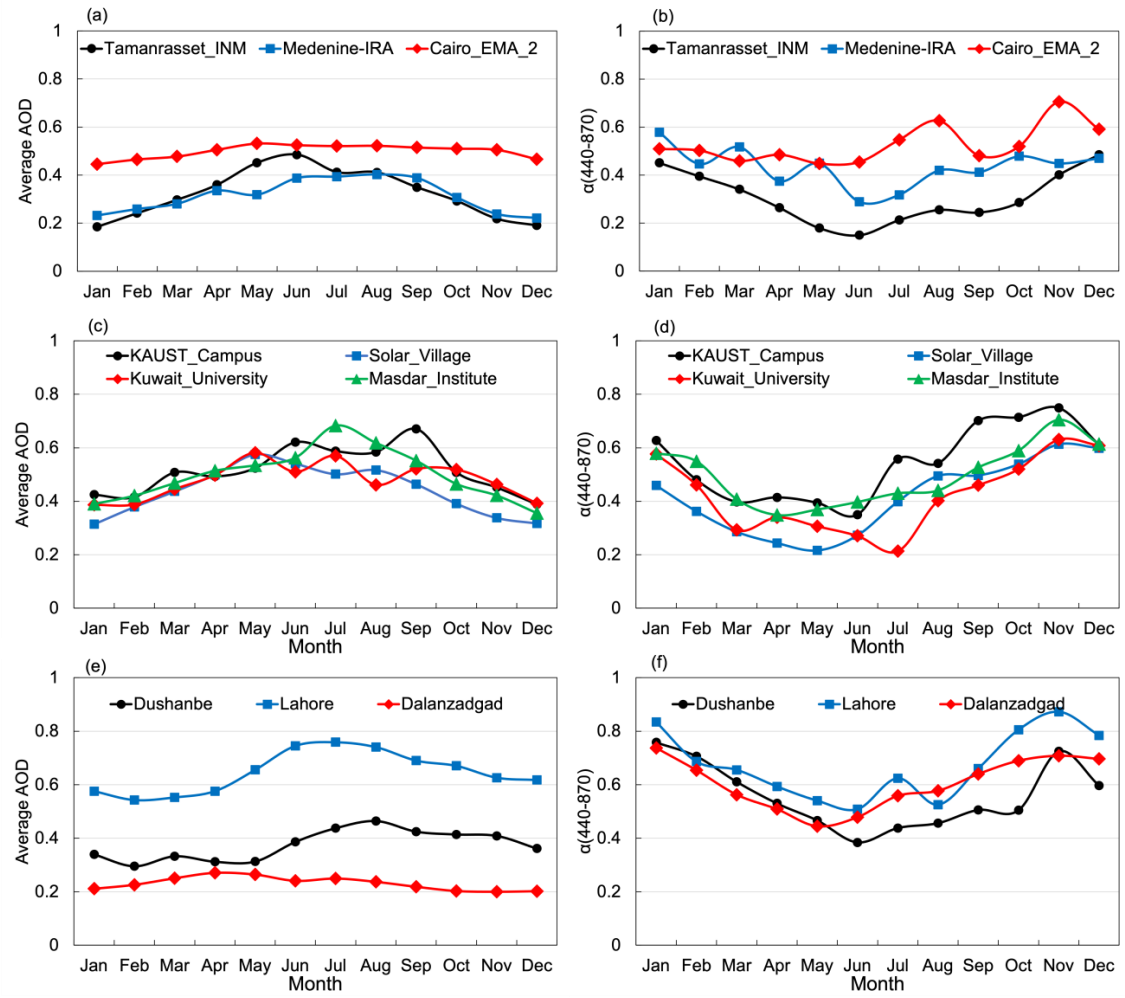

Figure 3. The average monthly AOD and Ångström exponent ($\alpha_{440\text{-}870}$) (**a**,**b**) for North African (Tamanrasset, Medenine, and Cairo), (**c**,**d**) for Middle Eastern (KASUT, Solar Village, Kuwait University, and the Masdar Institute), and (**e**,**f**) for Asian (Dushanbe, Lahore, and Dalanzadgad) AERONET stations.

Cairo, the location of the third AERONET station in the study area of North Africa, is the capital and largest city of Egypt, as well as one of the most populous cities in Africa and the Arab world. It is situated in the northern part of Egypt, along the banks of the Nile River. Cairo, as a major city, can experience the presence of aerosols in its atmosphere due to urban pollution, desert regions, and anthropogenic activities. The average annual AOD (Ångström exponent) value for the Cairo station is 0.50 (0.49) during the study period (2010–2019). It is evident from Figure 2a,b (red line) that, for the Cairo station, the highest value of annual AOD (Ångström exponent) is 0.53 (0.58) for the year 2018 (2011), while the lowest value of annual AOD (Ångström exponent) is 0.48 (0.38) for the

year 2012 (2013). It is noteworthy that the average AOD value for the Cairo station is significantly higher compared to those of the other two North African cities included in the study, and this value exhibits minimal variation over time. One reason for this is associated with the anthropogenic aerosols that can be present in Cairo's atmosphere throughout the year due to ongoing urban and industrial activities. Similarly, seasonal aerosol variations in Cairo are influenced by various factors, including weather patterns, local sources of aerosol particles, and regional climate conditions [22,47]. For example, spring in Cairo is characterized by relatively mild temperatures and lower humidity with sand and dust storms originating from desert regions (Sahara) that can lead to increased levels of coarse aerosol particles. Summer is the hottest and driest period, which can lead to the formation of secondary aerosols, including fine particulate matter through photochemical reactions and the transformation of pollutants that can increase aerosol concentration (both natural and anthropogenic sources). The aerosol level starts to decrease in autumn due to decreasing temperatures, lower levels of humidity, and fewer events of sand and dust storms. The reduction in aerosol level continues in winter, especially due to occasional rainfall. This is clearly evident when examining the average monthly AOD (with high-value) and Ångström exponent (with low-value) data for the Cairo station, as depicted by the red lines in Figure 3a,b, which signifies a conformity between the results and those of previous research [44,48].

4.1.2. Middle East

The average annual AOD and Ångström exponent ($\alpha_{440\text{-}870}$) for Middle Eastern AERONET stations (Sollar Village, KAUST, Kuwait University, and the Masdar Institute) are shown in Figure 2c,d, while the average monthly AOD and Ångström exponent ($\alpha_{440\text{-}870}$) for the same stations are shown in Figure 3c,d. The average annual AOD (Ångström exponent) value for the Solar Village station is 0.45 (0.38) during the study period (1999–2013). It is evident from Figure 2c,d (blue line) that, for the Solar Village station, the highest value of annual AOD (Ångström exponent) is 0.54 (0.53) for the year 2011 (1999), while the lowest value of annual AOD (Ångström exponent) is 0.37 (0.32) for the year 2001 (2013). In the Solar Village, with mild to warm temperatures and relatively low humidity during the spring season, sand and dust storms originating from the surrounding desert regions, including the Rub' al Khali Desert (Empty Quarter), can lead to elevated levels of coarse aerosol particles in the atmosphere. The increase in aerosol particles continues into summer, with extremely hot and dry conditions. The concentration of aerosols, however, decreases in the autumn and winter seasons due to the gradually decreasing temperature, occasional rainfall, and decreased frequency of sand and dust storm events [22,49]. This pattern is evident when analyzing the monthly AOD variability of the Solar Village (blue line in Figure 3c), where the concentration of aerosols starts increasing from March to June and becomes stable during July and August before decreasing in the following months. The spring months, from March to May, often see an increase in the concentration of aerosols. This is clearly evident when examining the average monthly AOD (with high-value) and Ångström exponent (with low-value) data for the Solar Village station, as depicted by the blue lines in Figure 3c,d, which is in agreement with the results of previous research [24,50].

The average annual AOD (Ångström exponent) value for the KAUST station is 0.47 (0.54) during the study period (2012–2023). It is evident from Figure 2c,d (black line) that, for the KAUST station, the highest value of annual AOD (Ångström exponent) is 0.57 (0.79) for the year 2017 (2016), while the lowest value of annual AOD (Ångström exponent) is 0.23 (0.33) for the year 2022 (2015). KAUST, located on the Red Sea coast of Saudi Arabia, experiences distinct seasonal aerosol variations influenced by its climate, geography, and local sources of aerosols. For example, the spring season is characterized by warm and pleasant weather with gradually rising temperatures, having occasional sand and dust storms, especially in the early part of spring, while summer is hot and dry with high temperatures and low humidity. The combination of intense heat and arid conditions can lead to the formation of secondary aerosols, including fine particulate matter, thereby

increasing aerosol levels both due to natural and anthropogenic sources in summer. The autumn season is characterized by gradually decreasing temperatures, fewer sand and dust storms, and a subsequent decrease in aerosol concentrations in the atmosphere. On the other hand, winter is mild and comfortable, featuring cooler temperatures and occasional rainfall, which contribute to the reduction in aerosols in the atmosphere [22,49]. It is important to note that KAUST's coastal location along the Red Sea can have a moderating influence on its climate and aerosol levels in comparison to inland desert areas. The seasonal aerosol variation is also clearly evident when examining the average monthly AOD (with high-value) and Ångström exponent (with low-value) data for the KAUST station, as depicted by the black lines in Figure 3c,d, which indicates that the results align with what previous research has shown [24,50].

The average annual AOD (Ångström exponent) value for the Kuwait University station is 0.49 (0.41) during the study period (2006–2010 and 2019–2021). It is evident from Figure 2c,d (red line) that, for the Kuwait University station, the highest value of annual AOD (Ångström exponent) is 0.59 (0.64) for the year 2010 (2007), while the lowest value of annual AOD (Ångström exponent) is 0.39 (0.26) for the year 2007 (2008). The seasonal aerosol variations in Kuwait City, like in many other urban areas, are influenced by meteorological, climatic, and local factors. For example, sand and dust storms are common in the region in spring, which is responsible for the increase in coarse-mode aerosols. Aerosol levels tend to rise during summer due to several factors, including the intense heating of the desert surfaces, leading to the suspension of fine dust and sand particles, frequent sand and dust storms (known as Shamals) originating from the Arabian Desert, and stagnant air masses that can trap pollutants. In autumn, aerosol levels start to decline as temperatures become moderate, although dust storms can still occur, especially in September, but they become less frequent. Winter is relatively cool, with daytime temperatures in the mild to cool range and, thus, aerosol levels are generally lower [22]. The seasonal aerosol pattern is clearly evident when examining the average monthly AOD (with high-value) and Ångström exponent (with low-value) data for the Kuwait University station, as depicted by the red lines in Figure 3c,d, which is in agreement with the results of previous research [51].

The average annual AOD (Ångström exponent) value for the Masdar Institute station is 0.50 (0.45) during the study period (2012–2021). It is evident from Figure 2c,d (green line) that, for the Masdar Institute station, the highest value of annual AOD (Ångström exponent) is 0.58 (0.55) for the year 2012 (2019), while the lowest value of annual AOD (Ångström exponent) is 0.43 (0.33) for the year 2021 (2012). Masdar City, located in the United Arab Emirates, experiences seasonal aerosol variations similar to those in Kuwait City. In spring, there is a gradual increase in aerosol levels due to occasional sand and dust events. This increase is further elevated in summer due to the intense heating of the desert surface, the Shamal wind, and stagnant air masses. Similar to Kuwait City, the autumn and winter seasons in Masdar City witness lower levels of aerosols in the atmosphere [22]. The seasonal aerosols' variation is also clearly evident when examining the average monthly AOD (with high-value) and Ångström exponent (with low-value) data for the Masdar station, as depicted by the green lines in Figure 3c,d; these findings are aligned with those of prior research [52].

4.1.3. Asia

The average annual AOD and Ångström exponent ($\alpha_{440\text{-}870}$) for Asian AERONET stations (Dushanbe, Lahore, and Dalanzadgad) are shown in Figure 2e,f, while the average monthly AOD and Ångström exponent ($\alpha_{440\text{-}870}$) for the same stations are shown in Figure 3e,f. The average annual AOD (Ångström exponent) value for the Dushanbe station is 0.40 (0.49) during the study period (2010–2020). It is evident from Figure 2e,f (black line) that, for the Dushanbe station, the highest value of annual AOD (Ångström exponent) is 0.43 (0.56) for the year 2017 (2019), while the lowest value of annual AOD (Ångström exponent) is 0.35 (0.41) for the year 2015 (2010). Dushanbe, the capital city of

Tajikistan, experiences seasonal aerosol variations influenced by its geographical location and climatic conditions. For example, the aerosol levels in the city are relatively low during the spring season. The aerosol levels start increasing in summer and autumn due to a number of reasons, including dust and particulate matter from both local and regional sources becoming more prevalent due to dry conditions and occasional wind events, forest fires, and increased industrial activity. Aerosol levels, however, are lower during the winter months due to reduced dust activity and increased atmospheric stability [22]. The seasonal aerosols' variation is also clearly evident when examining the average monthly AOD (with high values from June to October) and Ångström exponent (with low values from June to October) data for the Dushanbe station, as depicted by the black lines in Figure 3e,f, which signifies a conformity between the results and those of previous research [53].

The average annual AOD (Ångström exponent) value for the Lahore station is 0.64 (0.62) during the study period (2006–2020). It is evident from Figure 2e,f (blue line) that, for the Lahore station, the highest value of annual AOD (Ångström exponent) is 0.70 (0.73) for the year 2009 (2008), while the lowest value of annual AOD (Ångström exponent) is 0.52 (0.54) for the year 2017 (2012). Lahore, the capital city of the Punjab province in Pakistan, experiences distinct seasonal variations in aerosol levels influenced by weather patterns, geography, and local sources of pollution. For example, in spring, the aerosol levels generally begin to increase due to occasional dust storms, while in summer, the dust and particulate matter from both local and regional sources can become more prevalent due to dry conditions and occasional wind events. Autumn is a transitional period when temperatures begin to cool and the air becomes more stable. Aerosol levels may vary but tend to be lower compared to the summer months. Agricultural activities, like crop burning, common in some areas around Lahore, can contribute to localized increases in aerosols during this season. In recent years, air pollutants, including particulate matter and gases, have been entering Lahore from China and India due to prevailing wind patterns during the winter months (particularly from November to February). Thus, winter, characterized by cool to cold temperatures, occasional fog, and smog events, tends to have elevated aerosols. In addition, temperature inversions, where a layer of warm air traps pollutants beneath a layer of cool air, can lead to the accumulation of aerosols. Particulate matter (PM2.5 and PM10) concentrations are often higher during this season, contributing to reduced visibility and health concerns [54]. This pattern of aerosol variability is clearly evident when examining the average monthly AOD (with high-value) and Ångström exponent (with low-value) data for the Lahore station, as depicted by the blue lines in Figure 3e,f; these findings are aligned with those of prior research [53,54].

The average annual AOD (Ångström exponent) value for the Dalanzadgad station is 0.23 (0.58) during the study period (1998–2022). It is evident from Figure 2e,f (red line) that, for the Dalanzadgad station, the highest value of annual AOD (Ångström exponent) is 0.25 (0.74) for the year 2019 (2016), while the lowest value of annual AOD (Ångström exponent) is 0.21 (0.45) for the year 2018 (1998). Dalanzadgad, located in the South Gobi Desert region of Mongolia, experiences distinctive seasonal aerosol variations due to its desert climate and geographical location. Dalanzadgad region is susceptible to dust events, especially during the spring and early summer, which can result in significant increases in aerosol levels. For example, aerosol levels start to rise in the spring as the melting of snow and ice exposes surfaces that may release dust and particulate matter. In addition, local agricultural activities, such as plowing and tilling fields, can also contribute to increased aerosols during spring. Similarly, during summer, in addition to occasional dust storms, wildfires in the surrounding areas can lead to elevated aerosol concentrations. In autumn, aerosol levels may remain relatively low, but there can be occasional fluctuations due to changes in vegetation, agricultural activities, and regional influences. The city experiences relatively low aerosol levels during the winter months. In addition, snowfall and frozen ground help to reduce the resuspension of dust and particulate matter. However, occasional dust storms originating from nearby desert regions, such as the Gobi Desert, can lead to short-term increases in aerosol concentrations [22,55]. The seasonal aerosol variation is

also clearly evident when examining the average monthly AOD (with high values from February to June) and Ångström exponent (with low values from February to June) data for the Dalanzadgad station, as depicted by the red lines in Figure 3e,f, which is in agreement with the results of previous research [55].

4.2. AODs and Ångström Exponent Relationship

Specifically, scatter plots involving AODs and the Ångström exponent ($\alpha_{440\text{-}870}$) have been created to obtain insights into the composition and characteristics of the aerosols present in a particular geographic region [37,56,57]. These scatter plots reveal patterns or clusters of data points. Each cluster represents a distinct aerosol type or category, and the physical interpretation of these clusters is the key to identify the aerosols' characteristics. The AOD is a critical parameter that measures the extent to which aerosols in the atmosphere scatter or absorb sunlight at specific wavelengths. It provides a quantitative measure of the aerosol concentration in the atmosphere at that wavelength. However, the AOD alone does not provide information about the nature or type of aerosols present. This is where the Ångström exponent becomes relevant. Different aerosol types, such as fine urban pollution, coarse desert dust, or biomass-burning particles, exhibit distinct Ångström exponent values due to variations in their size, composition, and scattering properties.

In the current study, the scatter plots between AODs (500 nm) and the Ångström exponent ($\alpha_{440\text{-}870}$) for North Africa, Middle East, and Asia, as shown in Figure 4a–c, were analyzed. Kaskaoutis et al. (2007) [38] used the scatter plots of AOD (500 nm) and Ångström exponent (α440-870) data from four different AERONET stations to distinguish between various aerosol types. In the classification process, they applied threshold values from [58] and categorized the aerosols into four groups. In this study, we applied [38] classification scheme to the scatter plots (Figure 4a–c) of 10 AERONET stations in the dust belt region to classify aerosols into four groups, that is, clean maritime (if AOD < 0.06 and $\alpha_{440\text{-}870} < 1.3$), biomass burning (if AOD > 0.1 and $\alpha_{440\text{-}870} > 1.5$), desert dust (if AOD > 0.15 and $\alpha_{440\text{-}870} < 0.5$), and mixed aerosols (remaining). The percentage of each aerosol category extracted from the scatter plot information (Figure 4a–c) for the individual AERONET stations in the study area is shown in Figure 5.

The scatter plot between AODs (500 nm) and Ångström exponent (α440-870) data for the Tamanrasset AERONET station is shown in Figure 4a (blue dots). The analysis of the scatter plot data indicates that the Tamanrasset AERONET station has 0% of clean maritime aerosols, 0.3% of biomass-burning aerosols, 68% of desert dust aerosols, and 31.7% of mixed aerosols (Figure 5). Considering the geography of Tamanrasset city, there is some anthropogenic contribution, but the major contribution of atmospheric aerosols is from the great Sahara Desert, as 68% of the total data corresponds to desert dust aerosols. Similarly, analyzing the scatter plot for the Medenine AERONET station (orange dots in Figure 4a) indicates that there is 0% of clean maritime aerosols, 5% of biomass-burning aerosols, 37% of desert dust aerosols, and 58% of mixed aerosols (Figure 5). Medenine city is situated approximately 20 km from the Mediterranean coast, in southern Tunisia. It is important to note that, while the major source of aerosols is the Sahara Desert, its proximity to the coast leads to elevated humidity levels that may potentially influence aerosol dynamics.

For the Cairo AERONET station (green dots in Figure 4a), there is a 0% of clean maritime aerosols, 2% of biomass-burning aerosols, 13% of desert dust aerosols, and 85% of mixed aerosols (Figure 5). This is typical of a very large metropolitan city situated at the edge of the Nile Delta (which makes it a rich agricultural land), surrounded by desert regions, and serving as a major transportation hub for the region. The rise in Ångström exponent values as the AOD increases signifies the notable presence of fine 'fresh-smoke' particles in the atmospheric column, particularly in conditions of high turbidity. A comparable correlation between particle concentration (measured by the AOD) and particle size (assessed through the Ångström exponent) has been noted for various fine-mode aerosols [56,59,60]. These scenarios involve a blend of aerosol types, creating challenges in further characterizing urban and industrial aerosols. This complexity arises from the

interplay of various natural and human-related factors, such as relative humidity, cloud cover, altitude, fuel types, and emission characteristics, all of which affect aerosol formation and behavior. A similar behavior is evident from the scatter plot of Cairo city, where 85% of the total data shows mixed aerosols.

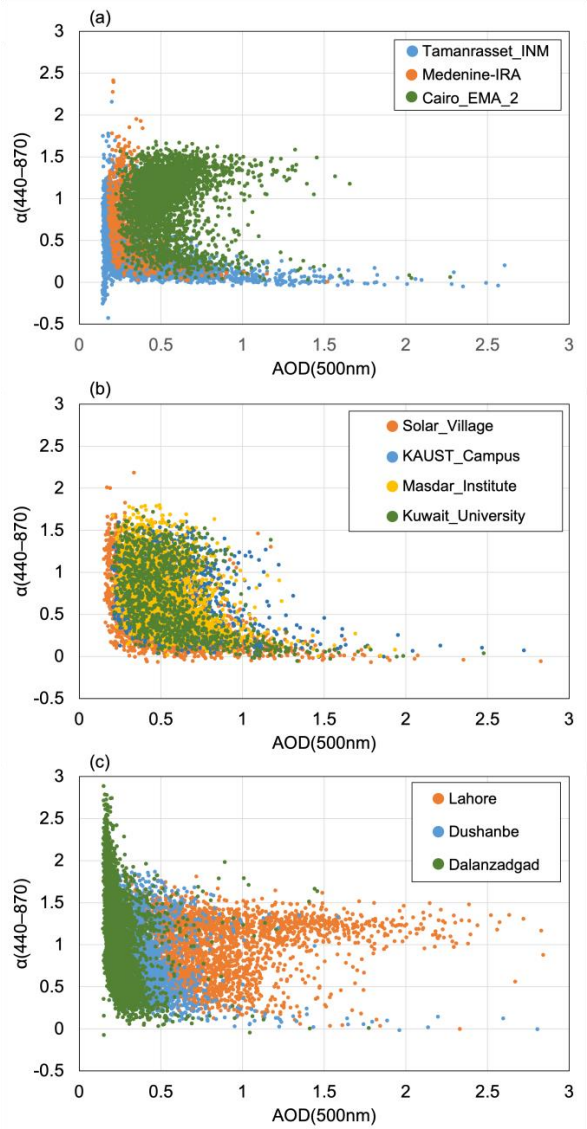

Figure 4. Scatter plots between AODs (500 nm) and the Ångström exponent ($\alpha_{440\text{-}870}$) for (**a**) North African (Tamanrasset, Medenine, and Cairo), (**b**) Middle Eastern (KASUT, Solar Village, Kuwait University, and the Masdar Institute), and (**c**) Asian (Dushanbe, Lahore, and Dalanzadgad) AERONET stations.

The scatter plot between the AOD (500 nm) and Ångström exponent ($\alpha_{440\text{-}870}$) data for the Solar Village AERONET station is shown in Figure 4b (orange dots). It must be noted that a similar pattern is evident from the analysis of all the AERONET stations in the Middle East. Therefore, a brief explanation is provided after the data from four stations are analyzed. The analysis of the scatter plot data indicates that the Solar Village AERONET station has 0% of clean maritime aerosols, 0.7% of biomass-burning aerosols, 50% of desert dust aerosols, and 49.3% of mixed aerosols (Figure 5). The scatter plot for the KAUST station (blue dots in Figure 4b) indicates that there is 0% of clean maritime aerosols, 0.6% of biomass-burning aerosols, 35% of desert dust aerosols, and 64.4% of mixed aerosols (Figure 5). For the Kuwait University AERONET station (green dots in Figure 4b), there is 0% of clean maritime aerosols, 2% of biomass-burning aerosols, 40% of

desert dust aerosols, and 58% of mixed aerosols (Figure 5). Finally, for the Masdar Institute AERONET station (yellow dots in Figure 4b), there is 0% of clean maritime aerosols, 4% of biomass-burning aerosols, 33% of desert dust aerosols, and 63% of mixed aerosols (Figure 5). It must be noted that all four stations in the Middle East are known for their arid desert climate with aerosol contributions from sand and dust storms, construction, industrial processes, and energy production. In addition, biomass burning occurs in the region and contributes to the anthropogenic aerosol concentration. In more specific terms, when analyzing the scatter plot of Figure 4b, a wide range of Ångström exponent values, spanning from approximately 0.1 to 1.6, is observed for moderate-to-low AODs (<0.5). However, for larger AOD values ($\geq$0.5), the Ångström exponent consistently falls below 0.5. This indicates the prevalence of coarse particles, which are characteristic of dust aerosols. The predominant presence of large particles with a radius greater than 0.6 μm distinguishes the optical properties of dust from the fine-mode-dominated aerosols produced by biomass burning and urban/industrial sources. In these AERONET station locations (specifically for the Solar Village), coarse-mode particles have the potential to mix with pollution aerosols originating from nearby industrialized regions in the Arabian Gulf or with smoke generated by oil fires (as discussed in Smirnov et al., 2002). This combination has been documented [61,62] to alter the wavelength dependence of the AOD and significantly influence the spectral single-scattering albedo.

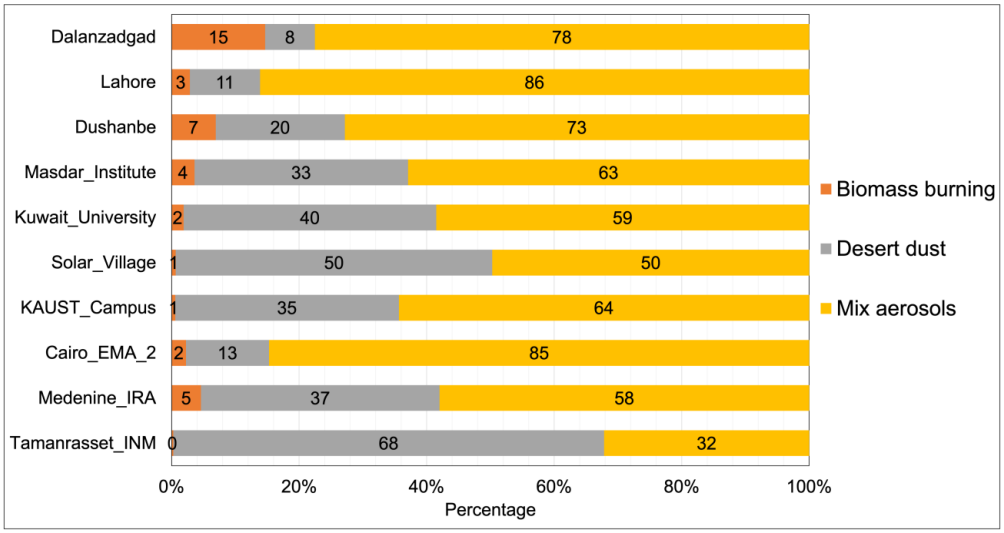

Figure 5. Percentage of aerosol types for each station.

The scatter plot between AODs (500 nm) and Ångström exponent ($\alpha_{440\text{-}870}$) data for the Dushanbe AERONET station is shown in Figure 4c (blue dots). Once again, since all three stations in Asia have more or less a similar pattern, a brief explanation is provided after the data are analyzed. The analysis of the scatter plot data indicates that the Dushanbe AERONET station has 0% of clean maritime aerosols, 7% of biomass-burning aerosols, 20% of desert dust aerosols, and 73% of mixed aerosols (Figure 5). Similarly, analyzing the scatter plot for Lahore AERONET station (orange dots in Figure 4c) indicates that there is 0% of clean maritime aerosols, 3% of biomass-burning aerosols, 11% of desert dust aerosols, and 86% of mixed aerosols (Figure 5). For the Dalanzadgad AERONET station (green dots in Figure 4c), there is 0% of clean maritime aerosols, 15% of biomass-burning aerosols, 8% of desert dust aerosols, and 77% of mixed aerosols (Figure 5).

Both Dushanbe (located in a mountainous region) and Lahore (in proximity of the Ravi River) are metropolitan cities that undergo construction, transportation, and industrial activities all year round. On the other hand, although Dalanzadgad is situated in the Gobi Desert region of southern Mongolia, the city is highly affected by the ongoing mining activities that enhance the aerosol concentration in the atmosphere. The presence of a high percentage of mixed aerosols for these locations is clearly evident in the scatter plot.

An analogous relationship between particle concentration, as determined by AODs, and particle size, assessed through the Ångström exponent, has been observed for a range of fine-mode aerosols [56,59,60]. These instances correspond to mixed aerosols, making it challenging to further characterize urban/industrial aerosols. This complexity arises from the intricate interplay of natural and anthropogenic factors, including relative humidity, cloud cover, altitude, fuel types, and emission characteristics, all of which influence aerosol formation and evolution, a pattern that is evident in Figure 4c.

4.3. Relationship of AODs and Meteorological Parameters

This study also investigated the relationship between daily AOD and a range of meteorological parameters, including temperature, visibility, relative humidity, wind speed, and wind direction, and the results are presented in Table 3. Meteorological data were not available for Dalanzadgad and, therefore, the relationship was not investigated. Across all stations, the findings reveal that visibility exhibits the strongest correlation with AODs among the analyzed meteorological parameters. Specifically, at the Tamanrasset Institute, there is a robust negative correlation of −0.79, signifying that, as the AOD increases, visibility tends to decrease significantly. Conversely, the Masdar Institute demonstrates a weaker negative correlation of −0.27, suggesting that an increased AOD has a relatively smaller impact on visibility at this location. The temperature also shows a noteworthy relationship with AODs, with the Masdar Institute displaying the highest positive correlation of 0.52. On the other hand, Dushanbe demonstrates a weaker positive correlation of 0.08, implying that the temperature has a less pronounced effect on AODs in this region.

Table 3. The correlation coefficient between AODs and meteorological parameters.

Station	Temperature	Visibility	Relative Humidity	Wind Speed	Wind Direction
Tamanrasset	0.51	−0.79	0.12	0.17	0.02
Medenine	0.47	−0.33	0.00	0.29	−0.39
Cairo	0.08	−0.28	0.11	−0.21	0.08
KAUST	0.38	−0.36	0.13	0.01	0.04
Solar Village	0.35	−0.62	−0.21	0.21	−0.03
Kuwait University	0.30	−0.62	0.13	0.16	−0.13
Masdar Institute	0.52	−0.27	−0.28	0.24	−0.03
Dushanbe	0.08	−0.40	0.06	−0.10	0.17
Lahore	0.09	−0.47	0.36	0.00	−0.33
Dalanzadgad			No data		

The time series of AODs with visibility and the temperature are shown in Figures 6 and 7, respectively. Overall, with the increase in the AOD, the visibility decreases for all stations, except KAUST, which indicates a good agreement between the two parameters (Figure 6). On the other hand, there is a good agreement in the overall pattern of the temperature and the AOD for all stations. With the increase in the AOD, the temperature also increases for all stations, except KAUST and Solar Village (Figure 7). One possible reason for this disagreement is that the temperature and visibility data are not collected from the exact locations of the AERONET stations in KAUST and Solar Village. For instance, it is important to note that the meteorological data for KAUST are gathered from Jeddah, located about 90 km south of KAUST. Similarly, for the Solar Village, the meteorological data originate from Riyadh, which is approximately 50 km southeast of the Solar Village. This deviation is a key factor to consider in understanding the discrepancy, as environmental conditions can vary significantly over such distances. Nevertheless, the consistent agreement among AODs, visibility, and temperature across the stations highlights a strong correlation between these parameters, which can carry significant implications for air quality and human health. The analysis did not reveal strong correlations between AODs and other meteorological

parameters, such as wind speed, wind direction, and humidity, as indicated by the low correlation values. This inconsistency suggests that these parameters might be influenced by a broader array of factors, including local geography, microclimates, and various sources of aerosols.

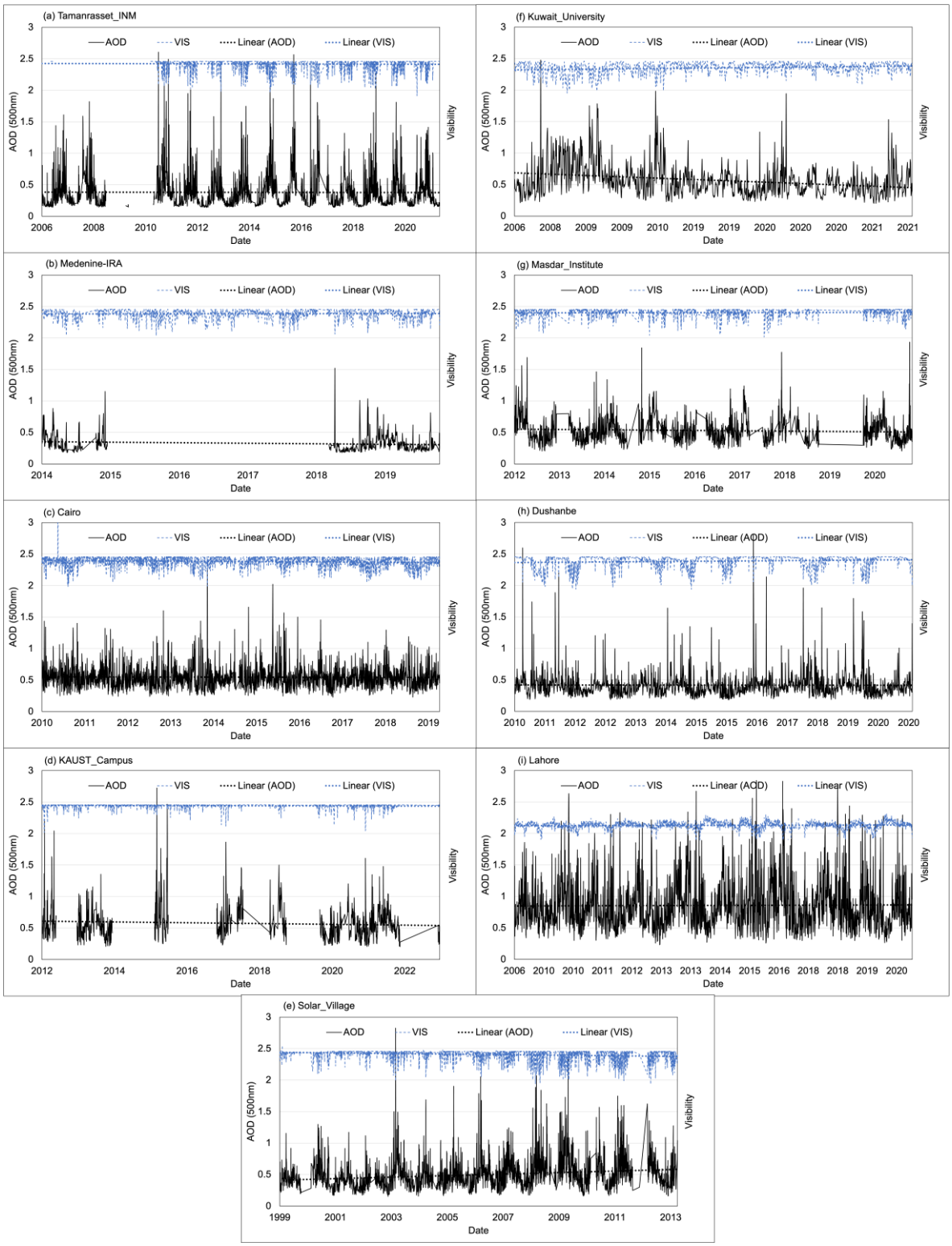

Figure 6. Daily AOD and visibility pattern for the AERONET stations.

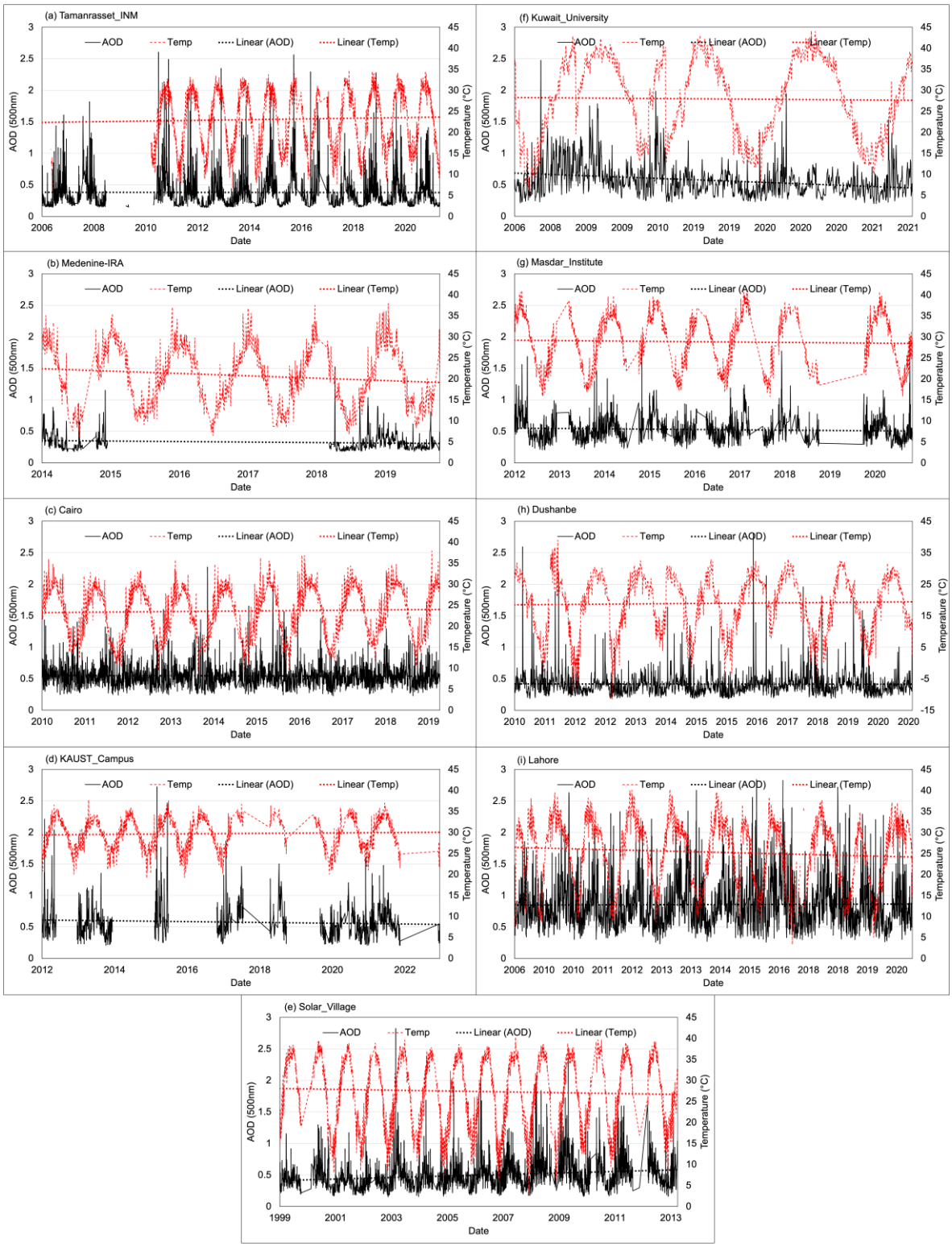

Figure 7. Daily AOD and temperature (°C) for the AERONET stations.

5. Conclusions

Detecting the short- and long-term changes in aerosols' loading/concentration has been the key area of research for climatologists and environmentalists in the world. In the monitoring atmospheric aerosol concentration (optical properties) using ground-based remote sensing techniques, AERONET is the largest network and is globally administered

by NASA. Since its first deployment, AERONET has been growing rapidly and a number of institutes have maintained long-term observations of aerosol data. The main feature of AERONET observational data (although they have limited spatial resolution) is their accuracy and high quality, which provide enough confidence to scientists to conduct aerosol-related research in different parts of the world. In addition, AERONET data have complemented and, in some applications, have been preferred to satellite remote-sensing-based observations in various studies. As the spectral behavior of the AOD is a key parameter in the study of atmospheric aerosols, influenced by both natural and anthropogenic processes, AERONET instruments capture AODs at multiple spectral bands, making them vital for understanding atmospheric aerosols.

The current research focused on the investigation of aerosol optical properties in the dust belt region. In summary, this study delved into the intricate realm of atmospheric aerosols, which are influenced by a multitude of factors, including sand and dust storms, anthropogenic emissions, geographic settings, and diverse aerosol properties. To comprehensively capture this diversity, data from ten strategically located AERONET stations were selected, offering insights into a wide range of atmospheric aerosol characteristics. These stations span diverse environments, encompassing arid deserts, coastal regions, bustling urban centers, and areas affected by biomass burning. For instance, locations like Dalanzadgad provided insights into natural aerosols typical of arid desert regions, while urban areas like Lahore and Dushanbe shed light on the complexities of anthropogenic aerosols stemming from urban activities. In the Middle East, stations like Solar Village, KAUST, Kuwait University, and the Masdar Institute collectively represent the climatic and geographical diversity of the region. Additionally, North African stations added a further complexity, with Cairo, Medenine, and Tamanrasset showcasing the unique features of bustling metropolises, coastal locations, and arid desert climates. Together, these stations provide a diverse array of insights into aerosol dynamics across various climates, geographies, and anthropogenic influences, enhancing our understanding of this complex phenomenon. Thus, the main objective of the current study was to generate, explain, and evaluate aerosol properties over the study area by utilizing AOD data at a 500 nm wavelength and Ångström exponent ($\alpha_{440\text{-}870}$). An approach was applied to differentiate between four distinct aerosol categories (maritime, biomass-burning, desert dust, and mixed aerosols). The analyses were conducted using daily aerosol data, and the findings are presented in terms of average monthly and annual values for each station. This comprehensive analysis aids in understanding aerosol dynamics across various regions and climatic conditions.

Based on the analysis conducted in this study, it was observed that the AERONET stations in North Africa (Tamanrasset, Medenine, and Cairo) exhibit varying patterns of aerosol concentrations. Tamanrasset experiences high turbidity annually from March to August due to the Saharan dust season. At the Medenine station, aerosol levels fluctuate with changing seasons, influenced by weather conditions and occasional dust storms. In contrast, Cairo consistently maintains higher aerosol levels throughout the year, primarily due to anthropogenic factors and urban activities. Cairo's aerosol patterns are also seasonally influenced by factors such as weather conditions and local sources, with elevated levels in spring and summer and decreased levels in autumn and winter. Similarly, among the Middle Eastern AERONET stations (Solar Village, KAUST, Kuwait University, and the Masdar Institute), the Solar Village and Masdar Institute exhibit distinct patterns, with elevated aerosol levels during the spring and summer that gradually decrease during the autumn and winter seasons. In contrast, KAUST and Kuwait University experience higher AOD levels in the summer due to intense heat, dry conditions, desert dust storms, and stagnant air masses. The Asian AERONET stations (Dushanbe, Lahore, and Dalanzadgad) exhibit distinct annual AOD (Ångström exponent) patterns. In Dushanbe, aerosol levels are lower during spring and increase in summer and autumn due to factors such as dry conditions, wind events, and industrial activities, while winter sees reduced aerosol levels. Lahore displays notable seasonal variations: spring marks the start of increased aerosols

due to occasional dust storms, summer experiences higher aerosol levels due to local and regional dust sources, autumn offers stabilization, and winter introduces elevated aerosols due to factors like temperature inversions and pollutants from neighboring regions. Dalanzadgad undergoes significant seasonal aerosol variations: spring sees rising aerosol levels from melting snow, local agriculture, and dust events; summer has occasional dust storms and wildfires; autumn is relatively stable; and winter exhibits low aerosol levels, with occasional dust storms.

In this study, scatter plots of AODs (500 nm) and Ångström exponent ($\alpha_{440\text{-}870}$) were employed to understand the composition and characteristics of aerosols in different geographic regions. These plots show clusters of data points, with each cluster representing a distinct aerosol type. These plots classified aerosols into four categories: clean maritime, biomass burning, desert dust, and mixed type. The percentages of each aerosol category for the specific AERONET stations in the study area were determined. For North African stations, Tamanrasset exhibited a dominance of desert dust aerosols. Medenine showed a mixture of desert dust and mixed aerosols due to its proximity to the coast. Cairo had a predominantly mixed aerosol composition due to its urban and industrial activities. In the Middle East, Solar Village, KAUST, Kuwait University, and the Masdar Institute shared a similar pattern, characterized by desert dust and mixed aerosols. In Asia, Dushanbe and Lahore displayed a high percentage of mixed aerosols, influenced by year-round urban and industrial activities. Dalanzadgad in Mongolia also featured mixed aerosols due to ongoing mining activities. The analysis of scatter plots provides valuable insights into the nature and composition of aerosols in various regions, reflecting the complex interplay of natural and anthropogenic factors. A strong correlation between AODs and visibility, as well as temperature, demonstrates a significant relationship, albeit with variations across different stations. Time-series data further revealed a consistent trend of reduced visibility with the increase in the AOD, except for KAUST. Simultaneously, a rise in temperature is observed with an increase in AOD levels, except for KAUST and Solar Village. The discrepancy in KAUST and Solar Village underscores the need for precise, location-specific meteorological data. In contrast, weak correlations between AODs and other meteorological parameters, such as wind speed, wind direction, and humidity, suggest that their influence is shaped by a broader range of factors, emphasizing the need for context-specific data. This research provides essential insights into the complex relationship between aerosols and their environmental context, with implications for air quality management and climate studies. In addition, the percentage change (Table 2) in annual AOD is also important as it allows researchers to track and quantify variations in aerosol concentrations over time, which, in turn, contributes to our understanding of environmental and climatic changes and their potential implications for society and the planet.

Author Contributions: Conceptualization, M.J.B. and A.E.S.; methodology, M.J.B.; software, A.E.S.; validation, M.J.B.; formal analysis, M.J.B.; investigation, A.E.S.; resources, A.E.S.; data curation, A.E.S.; writing—original draft preparation, A.E.S.; writing—review and editing, M.J.B.; visualization, A.E.S.; supervision, M.J.B.; All authors have read and agreed to the published version of the manuscript.

Funding: This research received no external funding.

Institutional Review Board Statement: Not applicable.

Informed Consent Statement: Not applicable.

Data Availability Statement: Restrictions apply to the availability of these data. Data was obtained from and are available at http://aeronet.gsfc.nasa.gov (accessed on 17 August 2023).

Acknowledgments: We would like to express our gratitude to the Goddard Earth Sciences Data and Information Services Center (GES DISC) for providing AERONET data. In this regard, all the AERONET Principal Investigators (PIs) have been duly notified and acknowledged for granting permission to use their data.

Conflicts of Interest: The authors declare no conflict of interest.

References

1. Finlayson-Pitts, B.; Pitts, J. *Chemistry of the Upper and Lower Atmosphere*; Elsevier: Amsterdam, The Netherlands, 2000. [CrossRef]
2. IPCC. *Climate Change 2007: Synthesis Report. Contribution of Working Groups I, II and III to the Fourth Assessment Report of the Intergovernmental Panel on Climate Change*; Pachauri, R.K., Reisinger, A., Eds.; IPCC: Geneva, Switzerland, 2007; p. 104.
3. IPCC. IPCC Special Report on Climate Change, Desertification, Land Degradation, Sustainable Land Management, Food Security, and Greenhouse Gas Fluxes in Terrestrial Ecosystems. 2019. Available online: https://www.ipcc.ch/srccl/ (accessed on 3 February 2021).
4. Streets, D.G.; Yan, F.; Chin, M.; Diehl, T.; Mahowald, N.; Schultz, M.; Wild, M.; Wu, Y.; Yu, C. Anthropogenic and natural contributions to regional trends in aerosol optical depth, 1980–2006. *J. Geophys. Res. Atmos.* **2009**, *114*, D00D18. [CrossRef]
5. Wild, M. Global dimming and brightening: A review. *J. Geophys. Res. Atmos.* **2009**, *114*, D00D16. [CrossRef]
6. Wang, S.; Fang, L.; Gu, X.; Yu, T.; Gao, J. Comparison of aerosol optical properties from Beijing and Kanpur. *Atmos. Environ.* **2011**, *45*, 7406–7414. [CrossRef]
7. Prospero, J.M.; Ginoux, P.; Torres, O.; Nicholson, S.E.; Gill, T.E. Environmental characterization of global sources of atmospheric soil dust identified with the Nimbus 7 Total Ozone Mapping Spectrometer (TOMS) absorbing aerosol product. *Rev. Geophys.* **2002**, *40*, 1002. [CrossRef]
8. Tehrani, N.A.; Farhanj, F.; Janalipour, M. Introducing a novel dust source identification method based on edge points and paths extracted from integration of time-series MODIS products. *Remote Sens. Appl. Soc. Environ.* **2023**, *32*, 101054. [CrossRef]
9. Boloorani, A.D.; Samany, N.N.; Papi, R.; Soleimani, M. Dust source susceptibility mapping in Tigris and Euphrates basin using remotely sensed imagery. *CATENA* **2022**, *209*, 105795. [CrossRef]
10. Asutosh, A.; Pandey, S.K.; Vinoj, V.; Ramisetty, R.; Mittal, N. Assessment of recent changes in dust over south asia using regcm4 regional climate model. *Remote Sens.* **2021**, *13*, 4309. [CrossRef]
11. Li, L.; Sokolik, I.N. Developing a Dust Emission Procedure for Central Asia. *Air Soil Water Res.* **2017**, *10*. [CrossRef]
12. Liu, X.; Zhang, Y.; Yao, H.; Lian, Q.; Xu, J. Analysis of the Severe Dust Process and Its Impact on Air Quality in Northern China. *Atmosphere* **2023**, *14*, 1071. [CrossRef]
13. Shi, L.; Zhang, J.; Yao, F.; Zhang, D.; Guo, H. Drivers to dust emissions over dust belt from 1980 to 2018 and their variation in two global warming phases. *Sci. Total Environ.* **2021**, *767*, 144860. [CrossRef] [PubMed]
14. Bouaziz, M.; Guermazi, H.; Khcharem, K.; Meszner, S.; Sarbeji, M.M. Aerosol uncertainty assessment: An integrated approach of remote AQUA MODIS and AERONET data. *Arab. J. Geosci.* **2019**, *12*, 50. [CrossRef]
15. Galvin, C.D. *Sand Dunes: Ecology, Geology and Conservation*; Nova Science Publishers, Inc.: New York, NY, USA, 2011.
16. Huneeus, N.; Schulz, M.; Balkanski, Y.; Griesfeller, J.; Prospero, J.; Kinne, S.; Bauer, S.; Boucher, O.; Chin, M.; Dentener, F.; et al. Global dust model intercomparison in AeroCom phase i. *Atmos. Chem. Phys.* **2011**, *11*, 7781–7816. [CrossRef]
17. Jin, Q.; Wang, C. The greening of Northwest Indian subcontinent and 1091 reduction of dust abundance resulting from Indian summer monsoon revival. *Sci. Rep.* **2018**, *8*, 4573. [CrossRef] [PubMed]
18. Qu, J.J.; Hao, X.; Kafatos, M.; Wang, L. Asian dust storm monitoring combining terra and aqua MODIS SRB measurements. *IEEE Geosci. Remote Sens. Lett.* **2006**, *3*, 484–486. [CrossRef]
19. Xu, D.; Qu, J.J.; Niu, S.; Hao, X. Sand and dust storm detection over desert regions in china with MODIS measurements. *Int. J. Remote Sens.* **2011**, *32*, 9365–9373. [CrossRef]
20. Middleton, N. Variability and trends in dust storm frequency on decadal timescales: Climatic drivers and human impacts. *Geosciences* **2019**, *9*, 261. [CrossRef]
21. Shao, Y.; Klose, M.; Wyrwoll, K.-H. Recent global dust trend and connections to climate forcing. *J. Geophys. Res. Atmos.* **2013**, *118*, 11107–11118. [CrossRef]
22. Goudie, A.S.; Middleton, N.J. *Desert Dust in the Global System*; Springer: Berlin/Heidelberg, Germany, 2006; pp. 1–287.
23. Buchard, V.; Da Silva, A.; Randles, C.; Colarco, P.; Ferrare, R.; Hair, J.; Hostetler, C.; Tackett, J.; Winker, D. Evaluation of the surface PM2.5 in Version 1 of the NASA MERRA Aerosol Reanalysis over the United States. *Atmos. Environ.* **2015**, *125*, 100–111. [CrossRef]
24. Butt, M.J.; Assiri, M.E.; Ali, M.A. Assessment of AOD variability over Saudi Arabia using MODIS Deep Blue products. *Environ. Pollut.* **2017**, *231*, 143–153. [CrossRef]
25. Li, Z.; Zhao, X.; Kahn, R.; Mishchenko, M.; Remer, L.; Lee, K.H.; Wang, M.; Laszlo, I.; Nakajima, T.; Maring, H. Uncertainties in satellite remote sensing of aerosols and impact on monitoring its long-term trend: A review and perspective. *Ann. Geophys.* **2009**, *27*, 2755–2770. [CrossRef]
26. Holben, B.N.; Eck, T.F.; Slutsker, I.; Tanré, D.; Buis, J.P.; Setzer, A.; Vermote, E.; Reagan, J.A.; Kaufman, Y.J.; Nakajima, T.; et al. AERONET—A federated instrument network and data archive for aerosol characterization. *Remote Sens. Environ.* **1998**, *66*, 1–16. [CrossRef]
27. Butt, M.J.; Mashat, A.S. MODIS satellite data evaluation for sand and dust storm monitoring in Saudi Arabia. *Int. J. Remote Sens.* **2018**, *39*, 8627–8645. [CrossRef]
28. Smirnov, A.; Holben, B.N.; Eck, T.F.; Dubovik, O.; Slutsker, I. Cloud-Screening and Quality Control Algorithms for the AERONET Database. *Remote Sens. Environ.* **2000**, *73*, 337–349. [CrossRef]
29. Shi, Y.; Zhang, J.; Reid, J.S.; Hyer, E.J.; Eck, T.F.; Holben, B.N.; Kahn, R.A. A critical examination of spatial biases between MODIS and MISR aerosol products—Application for potential AERONET deployment. *Atmos. Meas. Tech.* **2011**, *4*, 2823–2836. [CrossRef]

30. Belle, J.H.; Liu, Y. Evaluation of Aqua MODIS Collection 6 AOD Parameters for Air Quality Research over the Continental United States. *Remote Sens.* **2016**, *8*, 815. [CrossRef]
31. Wei, J.; Sun, L. Comparison and Evaluation of Different MODIS Aerosol Optical Depth Products over the Beijing-Tianjin-Hebei Region in China. *IEEE J. Sel. Top. Appl. Earth Obs. Remote Sens.* **2017**, *10*, 835–844. [CrossRef]
32. Kaskaoutis, D.G.; Prasad, A.K.; Kosmopoulos, P.G.; Sinha, P.R.; Kharol, S.K.; Gupta, P.; El-Askary, H.M.; Kafatos, M. Synergistic use of remote sensing and modeling for tracing dust storms in the mediterranean. *Adv. Meteorol.* **2012**, *2012*, 861026. [CrossRef]
33. Kim, D.; Chin, M.; Yu, H.; Eck, T.F.; Sinyuk, A.; Smirnov, A.; Holben, B.N. Dust optical properties over North Africa and Arabian Peninsula derived from the AERONET dataset. *Atmos. Chem. Phys.* **2011**, *11*, 10733–10741. [CrossRef]
34. Arola, A.; Schuster, G.; Myhre, G.; Kazadzis, S.; Dey, S.; Tripathi, S.N. Inferring absorbing organic carbon content from AERONET data. *Atmos. Chem. Phys.* **2011**, *11*, 215–225. [CrossRef]
35. Gregory, L. *Cimel Sunphotometer (CSPHOT) Handbook*; 2011. United States. Available online: https://www.osti.gov/servlets/purl/1020262 (accessed on 17 August 2021).
36. Cachorro, V.E.; Vergaz, R.; de Frutos, A.M. A quantitative comparison of α Ångströmturbidity parameter retrieved in different spectral ranges based on spectroradiometer solar radiation measurements. *Atmos. Environ.* **2001**, *35*, 5117–5124. [CrossRef]
37. Holben, B.N.; Tanre, D.; Smirnov, A.; Eck, T.F.; Slutsker, I. An emerging ground-based aerosol climatology: Aerosol optical depth from AERONET. *J. Geophys. Res.* **2001**, *106*, 12067–12097. [CrossRef]
38. Kaskaoutis, D.G.; Kambezidis, H.D.; Hatzianastassiou, N.; Kosmopoulos, P.G.; Badarinath, K.V.S. Aerosol climatology: On the discrimination of aerosol types over four AERONET sites. *Atmos. Chem. Phys. Discuss.* **2007**, *7*, 6357–6411. [CrossRef]
39. Eck, T.F.; Holben, B.N.; Reid, J.S.; Dubovik, O.; Smirnov, A.; O'Neill, N.T.; Slutsker, I.; Kinne, S. Wavelength dependence of the optical depth of biomass burning, urban, and desert dust aerosols. *J. Geophys. Res. Atmos.* **1999**, *104*, 31333–31349. [CrossRef]
40. Cachorro, V.E.; Vergaz, R.; De Frutos, A.M.; Vilaplana, J.M.; Henriques, D.; Laulainen, N.; Toledano, C. Study of desert dust events over the southwestern Iberian Peninsula in year 2000: Two case studies. *Ann. Geophys.* **2006**, *24*, 1493–1510. [CrossRef]
41. Schuster, G.L.; Dubovik, O.; Holben, B.N. Angstrom exponent and bimodal aerosol size distributions. *J. Geophys. Res. Atmos.* **2006**, *111*, 7207. [CrossRef]
42. Cuesta, J.; Edouart, D.; Mimouni, M.; Flamant, P.H.; Loth, C.; Gibert, F.; Marnas, F.; Bouklila, A.; Kharef, M.; Ouchène, B.; et al. Multiplatform observations of the seasonal evolution of the Saharan atmospheric boundary layer in Tamanrasset, Algeria, in the framework of the African Monsoon Multidisciplinary Analysis field campaign conducted in 2006. *J. Geophys. Res. Atmos.* **2008**, *113*, D23. [CrossRef]
43. Guirado, C.; Cuevas, E.; Cachorro, V.E.; Toledano, C.; Alonso-Pérez, S.; Bustos, J.J.; Basart, S.; Romero, P.M.; Camino, C.; Mimouni, M.; et al. Aerosol characterization at the Saharan AERONET site Tamanrasset. *Atmos. Chem. Phys.* **2014**, *14*, 11753–11773. [CrossRef]
44. Farahat, A. Comparative analysis of MODIS, MISR, and AERONET climatology over the Middle East and North Africa. *Ann. Geophys.* **2019**, *37*, 49–64. [CrossRef]
45. Abdulfattah, I.S.; Rajab, J.M.; Chaabane, M.; Lafta, M.H.; Lim, H.S. Air Surface Temperature Variability and Trends from Satellite Homogenized Time Series Data Over Tunis 2003–2021. In *IOP Conference Series: Earth and Environmental Science*; IOP Publishing: Bristol, UK, 2023. [CrossRef]
46. Choi, Y.; Chen, H.; Huang, C.; Earl, K.; Chen, Y.; Schwartz, C.S.; Matsui, T. Evaluating the Impact of Assimilating Aerosol Optical Depth Observations on Dust Forecasts Over North Africa and the East Atlantic Using Different Data Assimilation Methods. *J. Adv. Model. Earth Syst.* **2020**, *12*, e2019MS001890. [CrossRef]
47. Abdelaty, H.; Weiss, D.; Mangelkramer, D. Climate Policy in Developing Countries: Analysis of Climate Mitigation and Adaptation Measures in Egypt. *Sustainability* **2022**, *15*, 9121. [CrossRef]
48. Dawoud, W.; El Kenawy, A.M.; Abdel Wahab, M.M.; Oraby, A.H. Temporal Variability of Particulate Matter and Black Carbon Concentrations over Greater Cairo and Its Atmospheric Drivers. *Climate* **2023**, *11*, 133. [CrossRef]
49. Labban, A.H.; Butt, M.J. Analysis of sand and dust storm events over Saudi Arabia in relation with meteorological parameters and ENSO. *Arab. J. Geosci.* **2021**, *14*, 22. [CrossRef]
50. Albugami, S.; Palmer, S.; Meersmans, J.; Waine, T. Evaluating MODIS dust-detection indices over the Arabian Peninsula. *Remote Sens.* **2018**, *10*, 1993. [CrossRef]
51. Sabbah, I. Impact of aerosol on air temperature in Kuwait. *Atmos. Res.* **2010**, *97*, 303–314. [CrossRef]
52. Anoruo, C.M.; Bukhari, S.N.H.; Nwofor, O.K. Modeling and spatial characterization of aerosols at Middle East AERONET stations. *Theor. Appl. Climatol.* **2023**, *152*, 617–625. [CrossRef]
53. Rupakheti, D.; Rupakheti, M.; Rai, M.; Yu, X.; Yin, X.; Kang, S.; Orozaliev, M.D.; Sinyakov, V.P.; Abdullaev, S.F.; Sulaymon, I.D.; et al. Characterization of columnar aerosol over a background site in Central Asia. *Environ. Pollut.* **2022**, *316*, 120501. [CrossRef] [PubMed]
54. Khan, R.; Kumar, K.R.; Zhao, T. The climatology of aerosol optical thickness and radiative effects in Southeast Asia from 18-years of ground-based observations. *Environ. Pollut.* **2019**, *254*, 113025. [CrossRef]
55. Huang, G.; Zhou, Y.; Guo, Z.; Liu, X.; Chen, Y.; Liu, Q.; Ta, Z.; Wang, P.; He, Q.; Gao, J.; et al. The influence of dust aerosols on solar radiation and near-surface temperature during a severe duststorm transport episode. *Front. Environ. Sci.* **2023**, *11*, 1126302. [CrossRef]

56. Reid, J.S.; Eck, T.F.; Christopher, S.A.; Hobbs, P.V.; Holben, B.N. Use of the Angstrom exponent to estimate the variability of optical and physical properties of aging smoke particles in Brazil. *J. Geophys. Res.* **1999**, *104*, 27473–27489. [CrossRef]
57. Kaskaoutis, D.G.; Kambezidis, H.D. Investigation on the wavelength dependence of the 10 aerosol optical depth in the Athens area. *Q. J. R. Meteorol. Soc.* **2006**, *132*, 2217–2234. [CrossRef]
58. Pace, G.; di Sarra, A.; Meloni, D.; Piacentino, S.; Chamard, P. Aerosol optical properties at Lambeduca (Cenral Mediterranean). 1. Influence of transport and identification of different aerosol types. *Atmos. Chem. Phys.* **2006**, *6*, 697–713. Available online: http://www.atmos-chem-phys.net/6/697/2006/ (accessed on 17 August 2021). [CrossRef]
59. Porter, J.N.; Clarke, A.D. Aerosol size distribution models based on in situ measurements. *J. Geophys. Res.* **1997**, *102*, 6035–6045. [CrossRef]
60. Remer, L.A.; Kaufman, Y.; Holben, B.N.; Thompson, A.M.; McNamara, D.P. Biomass burning aerosol size distribution and modeled optical properties. *J. Geophys. Res.* **1998**, *103*, 31879–31891. [CrossRef]
61. Dubovik, O.; Holben, B.N.; Eck, T.F.; Smirnov, A.; Kaufman, Y.J.; King, M.D.; Tanre, D.; Slutsker, I. Variability of absorption and optical properties of key aerosol types observed in worldwide locations. *J. Atmos. Sci.* **2002**, *59*, 590–608. [CrossRef]
62. Smirnov, A.; Holben, B.N.; Dubovic, O.; O'Neil, N.T.; Eck, T.F.; Westphal, D.L.; Goroth, A.K.; Pietras, C.; Slutsker, I. Atmospheric aerosol optical properties in the Persian Gulf. *J. Atmos. Sci.* **2002**, *59*, 620–634. [CrossRef]